Available online at www.sciencedirect.com
ScienceDirect
International Journal of Thermal Sciences 46 (2007) 672–681
International Journal of Thermal Sciences
www.elsevier.com/locate/ijts

Meshless local Petrov–Galerkin approach for coupled radiative and conductive heat transfer

L.H. Liu *, J.Y. Tan

School of Energy Science and Engineering, Harbin Institute of Technology, 92 West Dazhi Street, Harbin 150001, People's Republic of China

Received 16 June 2006; received in revised form 19 September 2006; accepted 19 September 2006

Available online 23 October 2006

Abstract

A meshless local Petrov–Galerkin approach is employed for solving the coupled radiative and conductive heat transfer in absorbing, emitting and scattering media. The meshless local Petrov–Galerkin approach with upwind scheme for radiative transfer is based on the discrete ordinate equations. The moving least square approximation is used to construct the shape function. Three particular test cases for coupled radiative and conductive heat transfer are examined to verify this new approximate method. The dimensionless temperatures and the dimensionless heat fluxes are obtained. The results are compared with the other benchmark approximate solutions. By comparison, the results show that the meshless local Petrov–Galerkin approach has a good accuracy in solving the coupled radiative and conductive heat transfer in absorbing, emitting and scattering media.

Keywords: Radiation; Conduction; Combined heat transfer; Semitransparent medium; Meshless method

1. Introduction

Coupled radiative and conductive heat transfer in a semitransparent media is a problem of considerable practical importance in engineering applications. It serves as the basis, for example, in the analysis of the thermal performance of porous insulating materials such as fibers, powders, foams and many others. A solution of coupled radiative and conductive heat transfer involves two parts: the evaluation of the spatial distributions of the radiative energy source and the solution of the heat diffusion equation. Due to the mathematical complexity associated with radiation, some approximate methods are necessary for analysis of coupled radiative and conductive heat transfer in practical engineering.

Many approximation methods have been proposed to solve coupled radiative and conductive heat transfer in a semitransparent media. Viskanta and Grosh [1,2] analyzed numerically the problem of combined conduction radiation in a one-dimensional absorbing and emitting medium bounded by two parallel plates using an iterative method. Yuen and Wong [3] used a successive approximation technique to solve the heat transfer by conduction and radiation in a one-dimensional absorbing, emitting and anisotropically-scattering medium. Enoch et al. [4] presented a polynomial approximation solution of heat transfer by conduction and radiation in a one-dimensional absorbing, emitting, and scattering medium. Nice [5] studied a combined conductive–radiative heat transfer in one-dimensional semitransparent slab using finite element techniques. Burns et al. [6] analyzed numerically the problem of combined conduction radiation in a one-dimensional participating medium using a traditional Galerkin finite element method and the Swartz–Wendroff approximation. Yuen and Takara [7] analyzed a combined conductive–radiative heat transfer in two-dimensional rectangular enclosures by using a class of generalized exponential integral function. Razzaque et al. [8] employed the finite element method to solve a coupled conductive and radiative heat transfer in two-dimensional rectangular enclosures with gray participating media. Kim and Back [9] studied a coupled conductive and radiative heat transfer in two-dimensional rectangular enclosures, in which the central difference scheme was used to discretize the heat diffusion equation and the dis-

* Corresponding author. Tel.: +86 451 86402237; fax: +86 451 86221048.
E-mail address: lhliu@hit.edu.cn (L.H. Liu).

1290-0729/$ – see front matter
doi:10.1016/j.ijthermalsci.2006.09.005

Nomenclature

a	Coefficients for MLS approximation in Eq. (12)
$\mathbf{a}$	Vector of coefficient a
$\mathbf{A}$	Matrix defined in Eq. (15)
$\mathbf{B}$	Matrix defined in Eq. (16)
g	Scattering asymmetry factor
g_{qs}	Quartic spline functions
G	Dimensionless radiative intensity
G_w	Wall dimensionless radiative intensity
I	Radiative intensity
k	Order of monomial basis
k_c	Thermal conductivity
K	Coefficients in linear equations
M	Number of discrete ordinates for radiative transfer equation
n	Number of the nodes used for MLS approximation
n_w	Outward unit normal of boundary surface
$\mathbf{n}_w$	Outward unit normal vector of boundary surface
N	Number of scattered nodes in entire domain and its boundary
N_{CR}	Conduction to radiation parameter
$\mathbf{p}$	Monomial basis
q_x, q_y, q_z	Directional heat fluxes
Q_x, Q_y, Q_z	Dimensionless heat fluxes defined in Eqs. (40)–(42)
$\mathbf{s}_m$	Unit vector in the direction m
T	Temperature
T_{ref}	Reference temperature
u	Trial function
$\mathbf{u}$	Vector of trial function
v	Test function
v_{sh}	Shifted test function
V_S	Local sub-domain for weighted integration
$V_{\mathbf{x}}$	Domain of definition of MLS approximation for the trial function at $\mathbf{x}$
w^m	Weight corresponding to the direction m
w^{MLS}	MLS weight function
$\mathbf{x}$	Vector of optical location
$\mathbf{x}_Q$	Gaussian quadrature points

Greek symbols

$\alpha_{\mathrm{MLS}}, \alpha_{\mathrm{GQ}}$	Dimensionless size parameters
β	Extinction coefficient
Γ	Boundary of entire problem domain
ε_w	Wall emissivity
Θ	Dimensionless temperature
Θ_w	Wall dimensionless temperature
μ, η, ξ	Direction cosines
σ	Stefan–Boltzmann constant
τ_x, τ_y, τ_z	Optical thickness variables
τ_L	Optical width
ϕ	Shape function
Φ	Scattering phase function
ω	Single scattering albedo
Ω	Solid angle

crete ordinates method is adopted to solve the radiative transfer equation.

Recently, with the development of computer and computational technique, many numerical methods have been developed to solve the integro-differential radiative transfer equation in semitransparent media, for example, Monte Carlo method, zonal method, discrete ordinates method, finite volume method, finite element method and so on [10,11]. After solving the spatial distributions of the radiative energy source, heat diffusion equation can be solved by using finite difference method [12] or finite element method [13]. The combination of the methods stated above can be used to deal with the coupled radiative and conductive heat transfer in multi-dimensional complicated geometry. However, because the problem domain needs to be discretized into meshes, these traditional methods, especially the finite element method, suffer from drawbacks such as tedious meshing and re-meshing in problems of large deformations.

In the community of computational mechanics, many meshless methods have been proposed for the problem of computational mechanics to avoid the tedious meshing and re-meshing. Meshless method is used to establish a system of algebraic equations for whole problem domain without the use of a predefined mesh. Meshless method uses a set of nodes scattered within the problem domain and its boundaries. These scattered nodes do not form a mesh, which means that no information on the relationship between the nodes is required. Various methods belonging to this family are the element free Galerkin method, the meshless local Petrov–Galerkin (MLPG) method, the point interpolation method, the smoothed particle hydrodynamics method and so on [14–16]. Among these methods, MLPG method is a truly meshless method, which was originated by Atluri and Zhu [17] for the problem of computational mechanics. Recently, meshless methods were introduced into the community of heat transfer. Singh et al. [18] dealt with the transient and steady-state solution of two-dimensional heat transfer through the fins using a meshless element free Galerkin method. Liu [19,20] develop an MLPG method based on the discrete-ordinates equation for radiative heat transfer and extended it to solve the radiative heat transfer problems in semitransparent medium with graded refractive index. Liu et al. [21] applied the MLPG approach for coupled radiative and conductive heat transfer in one-dimensional graded index medium. Sadat [22] used a meshless collocation method to solve radiative transfer problems. Both the primitive and the even parity formulations of the discrete ordinates method have been considered. It was found that the meshless method based on the primitive formulation appeared to be unstable and lead to oscillatory results while the meshless method based on the even parity formulation was seen to be stable in all situations. Liu

and Tan [23] found that the MLPG solution for radiative heat transfer problems sometimes also suffers oscillatory behavior.

The treatment of this oscillatory needs to exam the characteristics of radiative transfer equation in detail. Consider radiative transfer in a semitransparent medium. Taking direction cosines in radiative transfer equation as velocity components in the corresponding coordinate directions, respectively, the first derivative of radiative intensity can be considered as a convection term. Therefore, radiative transfer equation is a special case of the general convection–diffusion equation [24]. It is well known that convection–diffusion equations are some of the most difficult problems to solve numerically. Sometimes, the presence of the convection terms may cause oscillatory behavior of solutions. This type of instability can occur in many numerical methods including finite difference method, finite element method and meshless method if no special stability treatment is taken. The key to overcome this problem is to effectively capture the upstream information. The so-called upwind scheme similar to that widely used in finite difference method was developed in meshless methods to solve the problems of fluid dynamics [25].

In this paper, we employ a MLPG method for solving the coupled radiative and conduction heat transfer in semitransparent participating media, in which the standard MLPG method is used for solving heat conduction equation, while an upwind scheme of MLPG method is specially applied for solving radiative heat transfer based on the discrete-ordinates equations. The moving least square approximation is used to construct the shape function. Three cases of coupled radiative and conductive heat transfer in semitransparent media are examined to verify this new solution method for the problems of coupled radiative and conductive heat transfer.

2. Mathematical formulation

2.1. Physical model and control equation

We consider a semitransparent gray medium enclosed by opaque diffuse walls. For a steady-state coupled radiative and conductive heat transfer with the first boundary condition, by using the discrete ordinate approximation the dimensionless energy equation and the dimensionless radiative transfer equation can be written as

$$\frac{\partial^2\Theta}{\partial\tau_x^2}+\frac{\partial^2\Theta}{\partial\tau_y^2}+\frac{\partial^2\Theta}{\partial\tau_z^2}=\frac{(1-\omega)}{N_{\mathrm{CR}}}\left(\Theta^4-\frac{1}{4}\sum_{m=1}^{M}G^m w^m\right) \tag{1}$$

$$\mu^m\frac{\partial G^m}{\partial\tau_x}+\eta^m\frac{\partial G^m}{\partial\tau_y}+\xi^m\frac{\partial G^m}{\partial\tau_z}=-G^m+\frac{1-\omega}{\pi}\Theta^4+\frac{\omega}{4\pi}\sum_{m'=1}^{M}G^{m'}\Phi^{m,m'}w^{m'}\quad m=1,2,\ldots,M \tag{2}$$

with boundary conditions

$$\Theta_\Gamma=\Theta_w \tag{3}$$

$$G_w^m=\frac{\varepsilon_w\Theta_w^4}{\pi}+\frac{1-\varepsilon_w}{\pi}\sum_{\mathbf{n}_w\cdot\mathbf{s}_{m'}>0}|\mathbf{n}_w\cdot\mathbf{s}_{m'}|G_w^{m'}w^{m'}\quad|\mathbf{n}_w\cdot\mathbf{s}_m|<0 \tag{4}$$

Here, the dimensionless temperature Θ, the optical thickness variable τ_x, τ_y and τ_z, the conduction-to-radiation parameter N_{CR}, and the dimensionless radiative intensity G are defined, respectively, as follows

$$\Theta=\frac{T}{T_{\mathrm{ref}}} \tag{5}$$

$$\tau_x=\beta x \tag{6}$$

$$\tau_y=\beta y \tag{7}$$

$$\tau_z=\beta z \tag{8}$$

$$N_{\mathrm{CR}}=\frac{k_c\beta}{4\sigma T_{\mathrm{ref}}^3} \tag{9}$$

$$G=\frac{I}{\sigma T_{\mathrm{ref}}^4} \tag{10}$$

In the expressions written above, ω is the single scattering albedo, Φ is the scattering phase function, ε_w is the wall emissivity, $\mathbf{n}_w$ is the outward unit normal vector of boundary surface, $\mathbf{s}_{m'}$ is the unit vector in the direction m', μ^m, η^m and ξ^m are the direction cosine, w^m is the weight corresponding to the direction m, β is the extinction coefficient, k_c is the thermal conductivity, I is the radiative intensity, and T_{ref} is the reference temperature. By removing the forward scattering from right side of Eq. (2) to the left side, the dimensionless radiative transfer equation can be rewritten as [26]

$$\mu^m\frac{\partial G^m}{\partial\tau_x}+\eta^m\frac{\partial G^m}{\partial\tau_y}+\xi^m\frac{\partial G^m}{\partial\tau_z}+\left(1-\frac{\omega}{4\pi}\Phi^{mm}w^m\right)G^m=\left(\frac{1-\omega}{\pi}\Theta^4+\frac{\omega}{4\pi}\sum_{m'=1,\ m'\neq m}^{M}G^{m'}\Phi^{m,m'}w^{m'}\right) \tag{11}$$

2.2. Moving least square approximation

In MLPG implementation, Moving Least Square (MLS) approximation [14–17] is employed for constructing shape functions. Consider a spatial sub-domain $V_{\mathbf{x}}$, the neighborhood of a point $\mathbf{x}$ and denoted as the domain of definition of MLS approximation for the trial function at $\mathbf{x}$, which is located within the problem domain. To approximate the distribution of function u in$V_{\mathbf{x}}$, over a number of local nodes $\{\mathbf{x}_i\}$, $i=1,2,\ldots,n$, the MLS approximant $\tilde{u}(\mathbf{x})$ of u, $\forall\mathbf{x}\in V_{\mathbf{x}}$, can be defined by

$$\tilde{u}=\sum_{j=0}^{k}p_j(\mathbf{x})a_j(\mathbf{x})=\mathbf{p}^T(\mathbf{x})\mathbf{a}(\mathbf{x}) \tag{12}$$

where $\mathbf{p}^T(\mathbf{x})=[p_1(\mathbf{x}),p_2(\mathbf{x}),\ldots,p_k(\mathbf{x})]$ is a complete monomial basis of order k, and $\mathbf{a}(\mathbf{x})$ is a vector containing coefficients $a_j(\mathbf{x})$, $j=1,2,\ldots,k$, which are functions of the spatial coordinates $\mathbf{x}=[\tau_x,\tau_y,\tau_z]^T$. The coefficient vector $\mathbf{a}(\mathbf{x})$ is de-

termined by minimizing a weighted discrete L_2 norm, defined as:

$$J\big[\mathbf{a}(\mathbf{x})\big] = \sum_{i=1}^{n} w_i^{\mathrm{MLS}}\big[\mathbf{p}^T(\mathbf{x}_i)\mathbf{a}(\mathbf{x}) - \tilde{u}_i\big]^2 \tag{13}$$

where $\mathbf{x}_i$ denotes the value of $\mathbf{x}$ at node i; $w_i^{\mathrm{MLS}}(\mathbf{x})$ is the MLS weight function associated with the node i, with $w_i^{\mathrm{MLS}}(\mathbf{x}) > 0$ for all $\mathbf{x}$ in the support of $w_i^{\mathrm{MLS}}(\mathbf{x})$; and n is the number of nodes in $V_{\mathbf{x}}$ for which the weight functions $w_i^{\mathrm{MLS}}(\mathbf{x}) > 0$. Here, $\tilde{u}_i$ in Eq. (13) is the fictitious nodal value, and not the nodal value of unknown trial function $\tilde{u}_i$ in general.

The stationary of J with respect to $\mathbf{a}(\mathbf{x})$ leads to the following linear relation between $\mathbf{a}(\mathbf{x})$ and $\hat{\mathbf{u}}$.

$$\mathbf{A}(\mathbf{x})\mathbf{a}(\mathbf{x}) = \mathbf{B}(\mathbf{x})\hat{\mathbf{u}} \tag{14}$$

where the matrices $\mathbf{A}(\mathbf{x})$, $\mathbf{B}(\mathbf{x})$ and $\hat{\mathbf{u}}$ are defined by

$$\mathbf{A}(\mathbf{x}) = \sum_{i=1}^{n} w_i^{\mathrm{MLS}}(\mathbf{x})\mathbf{p}(\mathbf{x}_i)\mathbf{p}^T(\mathbf{x}_i) \tag{15}$$

$$\mathbf{B}(\mathbf{x}) = \big[w_1^{\mathrm{MLS}}(\mathbf{x})\mathbf{p}(\mathbf{x}_1),\, w_2^{\mathrm{MLS}}(\mathbf{x})\mathbf{p}(\mathbf{x}_2),\, \ldots,\, w_n^{\mathrm{MLS}}(\mathbf{x})\mathbf{p}(\mathbf{x}_n)\big] \tag{16}$$

$$\hat{\mathbf{u}} = [\hat{u}_1, \hat{u}_2, \ldots, \hat{u}_n] \tag{17}$$

Solving for $\mathbf{a}(\mathbf{x})$ from Eq. (14) and substituting it into Eq. (12) gives a relation which may be written in the form of an interpolation function similar to that used in finite element method, as

$$\tilde{u}(\mathbf{x}) = \sum_{i=1}^{n} \phi_i(\mathbf{x})\hat{u}_i, \quad \forall \mathbf{x} \in V_{\mathbf{x}} \tag{18}$$

where

$$\phi_i(\mathbf{x}) = \sum_{j=1}^{k} p_j(\mathbf{x})\big[\mathbf{A}^{-1}(\mathbf{x})\mathbf{B}(\mathbf{x})\big]_{ji} \tag{19}$$

Here, $\phi_i(\mathbf{x})$ is usually called as the shape function of MLS approximation corresponding to nodal point $\mathbf{x}_i$. The partial derivatives of the shape function is obtained as

$$\phi_{i,l}(\mathbf{x}) = \sum_{j=1}^{k}\big\{p_{j,l}\big[\mathbf{A}^{-1}\mathbf{B}\big]_{ji} + p_j\big[\mathbf{A}^{-1}\mathbf{B}_{,l} + \big(\mathbf{A}^{-1}\big)_{,l}\mathbf{B}\big]_{ji}\big\}, \tag{20}$$

where $(\,)_{,l} = \partial(\,)/\partial l$ represents the derivative with respect to spatial coordinate l, $l = \tau_x, \tau_y, \tau_z$.

2.3. Standard MPLG and upwind scheme of the MPLG

The MLPG method is based on Petrov–Galerkin weighting procedures. Different spaces for the test and trial functions can be used. The quartic spline functions are often used to construct the weight function for the MLS approximation and test function in the weighted integration for the standard MLPG method. One of the often used quartic spline functions is given as follows [2]:

$$g_{\mathrm{qs}}(r) = \begin{cases} 1 - 6r^2 + 8r^3 - 3r^4, & r \leqslant 1 \\ 0, & r > 1 \end{cases} \tag{21}$$

where r is the dimensionless distance. In the standard MLPG method, the weight function $w^{\mathrm{MLS}}(\mathbf{x} - \mathbf{x}_i)$ for the MLS approximation and the test function $v(\mathbf{x} - \mathbf{x}_i)$ in the weighted integration can be constructed as follows:

$$w^{\mathrm{MLS}}(\mathbf{x} - \mathbf{x}_i) = g_{\mathrm{qs}}\left(\left|\frac{\tau_x - \tau_{x_i}}{\alpha_{\mathrm{MLS}}\Delta\tau_x}\right|\right) g_{\mathrm{qs}}\left(\left|\frac{\tau_y - \tau_{y_i}}{\alpha_{\mathrm{MLS}}\Delta\tau_y}\right|\right) \times g_{\mathrm{qs}}\left(\left|\frac{\tau_z - \tau_{z_i}}{\alpha_{\mathrm{MLS}}\Delta\tau_z}\right|\right) \tag{22}$$

$$v(\mathbf{x} - \mathbf{x}_i) = g_{\mathrm{qs}}\left(\left|\frac{\tau_x - \tau_{x_i}}{\alpha_{\mathrm{GQ}}\Delta\tau_x}\right|\right) g_{\mathrm{qs}}\left(\left|\frac{\tau_y - \tau_{y_i}}{\alpha_{\mathrm{GQ}}\Delta\tau_y}\right|\right) \times g_{\mathrm{qs}}\left(\left|\frac{\tau_z - \tau_{z_i}}{\alpha_{\mathrm{GQ}}\Delta\tau_z}\right|\right) \tag{23}$$

where $\Delta\tau_x$, $\Delta\tau_y$ and $\Delta\tau_z$ are the average nodal spacing between two neighboring nodes in the τ_x, τ_y and τ_z coordinate directions, respectively; α_{MLS} and α_{GQ} are dimensionless size parameters.

Because the quartic spline function defined in Eq. (21) is a symmetric compact support function, in the standard MLPG method, both the weight function $w^{\mathrm{MLS}}(\mathbf{x} - \mathbf{x}_i)$ for the MLS approximation and the test function $v(\mathbf{x} - \mathbf{x}_i)$ in the weighted integration capture the upwind and the downwind information equally. Therefore, one of the natural ways to construct upwind scheme is to choose different trial and test functions to effectively capture the upstream information. Lin and Atluri [25] choose a skewed weight function for the test function $v(\mathbf{x} - \mathbf{x}_i)$. As shown in Fig. 1, the position of the maximum of the normal test function is shifted $\mathbf{x}_i$ from to $\mathbf{x}'_i$ along the upwind direction. Following this way, for the radiative transfer along the direction $\mathbf{s}_m = \mathbf{i}\mu^m + \mathbf{j}\eta^m + \mathbf{k}\xi^m$, a upwind scheme of MLPG for radiative transfer equation can be set up by keeping the weight function $w^{\mathrm{MLS}}(\mathbf{x} - \mathbf{x}_i)$ same as Eq. (22), but shifting the position of the maximum of the test function along the right-about of radiative transfer direction as follows:

$$\tau'_{x_i} = \tau_{x_i} - c_s\mu^m\alpha_Q\,\Delta\tau_x \tag{24a}$$

$$\tau'_{y_i} = \tau_{y_i} - c_s\eta^m\alpha_Q\,\Delta\tau_y \tag{24b}$$

$$\tau'_{z_i} = \tau_{z_i} - c_s\xi^m\alpha_Q\,\Delta\tau_z \tag{24c}$$

where c_s is the shift parameter of the test function. After shifted, the test function in the weighted integration is changed as following

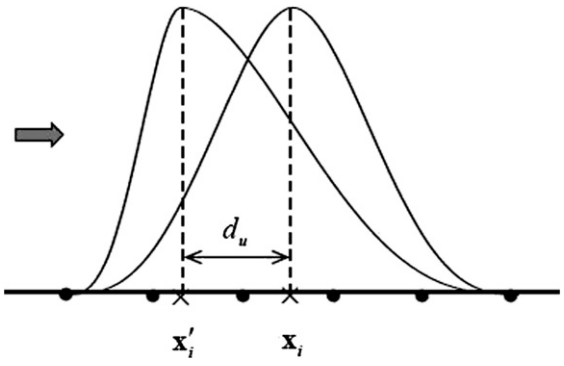

Fig. 1. Test function and its shift.

$$v_{\mathrm{sh}}(\mathbf{x}-\mathbf{x}_i) = g_{\mathrm{qs}}\left(\left|\frac{\tau_x-\tau_{x_i}+c_s\mu^m\alpha_{\mathrm{GQ}}\Delta\tau_x}{[1+\mathrm{sign}(\tau_x-\tau_{x_i})c_s\mu^m]\alpha_{\mathrm{GQ}}\Delta\tau_x}\right|\right) \times g_{\mathrm{qs}}\left(\left|\frac{\tau_y-\tau_{y_i}+c_s\eta^m\alpha_{\mathrm{GQ}}\Delta\tau_y}{[1+\mathrm{sign}(\tau_y-\tau_{y_i})c_s\eta^m]\alpha_{\mathrm{GQ}}\Delta\tau_y}\right|\right) \times g_{\mathrm{qs}}\left(\left|\frac{\tau_z-\tau_{z_i}+c_s\xi^m\alpha_{GQ}\Delta\tau_z}{[1+\mathrm{sign}(\tau_z-\tau_{z_i})c_s\xi^m]\alpha_{\mathrm{GQ}}\Delta\tau_z}\right|\right) \tag{25}$$

where $\mathrm{sign}(a)$ is a sign function defined as

$$\mathrm{sign}(a) = \begin{cases} 1, & a \geqslant 0 \\ -1, & a < 0 \end{cases} \tag{26}$$

The upwind scheme given by Eqs. (24) and (25) can be very easily implemented, and the optimum shift parameter $c_s = 0.5$ is recommended in Ref. [23].

2.4. Discretization and numerical implementation

The upwind scheme of MLPG method is used for solving radiative heat transfer based on the discrete-ordinates equations The dimensionless radiative transfer equation (11) is weighted using the shifted test function over the local sub-domain V_S, which is located entirely inside the global problem domain. The integrated residuals are set to zero

$$\int_{V_S}\left[\mu^m\frac{\partial G^m}{\partial\tau_x}+\eta^m\frac{\partial G^m}{\partial\tau_y}+\xi^m\frac{\partial G^m}{\partial\tau_z}+\left(1-\frac{\omega}{4\pi}\Phi^{mm}w^m\right)G^m - \left(\frac{1-\omega}{\pi}\Theta^4+\frac{\omega}{4\pi}\sum_{m'=1,\ m'\neq m}^{M}G^{m'}\Phi^{m,m'}w^{m'}\right)\right] \times v_{\mathrm{sh}}(\mathbf{x}-\mathbf{x}_i)\,\mathrm{d}V = 0 \quad i=1,2,\ldots,N \tag{27}$$

Here N is the total number of nodes. Substitution of Eqs. (18)–(20) into Eq. (27) for all nodes leads to the following discretized system of linear equations:

$$\sum_{j=1}^{N}K_{ij}^m G_j^m = f_i^m, \quad i=1,2,\ldots,N \tag{28}$$

where

$$K_{ij}^m = \int_{V_S}\left[\mu^m\phi_{j,x}(\mathbf{x})+\eta^m\phi_{j,y}(\mathbf{x})+\xi^m\phi_{j,z}(\mathbf{x}) + \left(\kappa+\sigma-\frac{\sigma}{4\pi}\Phi^{mm}w^m\right)\phi_j(\mathbf{x})\right]v_{\mathrm{sh}}(\mathbf{x}-\mathbf{x}_i)\,\mathrm{d}V \tag{29}$$

$$f_i^m = \int_{V_S}\left(\kappa I_b+\frac{\sigma}{4\pi}\sum_{m'=1,\ m'\neq m}^{M}G^{m'}\Phi^{m'm}w^{m'}\right) \times v_{\mathrm{sh}}(\mathbf{x}-\mathbf{x}_i)\,\mathrm{d}V \tag{30}$$

Eq. (28) is solved independently for each direction, and the boundary conditions must be imposed on the inflow boundary. For each node i on the inflow boundary, the dimensionless radiative intensity G_i^m is given by Eq. (4), and the boundary condition can be directly imposed as follows:

$$K_{ij}^m = \begin{cases} 1, & i=j \\ 0, & i\neq j \end{cases} \tag{31}$$

$$f_i^m = G_i^m \tag{32}$$

Because the in-scattering term in the discrete-ordinates equation at the direction m contains the radiative intensities of the other direction, the global iterations similar to that used in discrete-ordinates method are necessary to include the source and boundary conditions.

The standard MLPG method is used for solving heat conduction equation. The weighted integral form of the dimensionless energy equation is given as

$$\int_{V_S}\left[\frac{\partial^2\Theta}{\partial\tau_x^2}+\frac{\partial^2\Theta}{\partial\tau_y^2}+\frac{\partial^2\Theta}{\partial\tau_z^2}-\frac{(1-\omega)}{N_{\mathrm{CR}}}\left(\Theta^4-\frac{1}{4}\sum_{m=1}^{M}G^m w^m\right)\right] \times v(\mathbf{x}-\mathbf{x}_i)\,\mathrm{d}V = 0 \tag{33}$$

Using $v\nabla^2\Theta = \Theta_{,ll}v = (\Theta_{,l}v)_{,l} - \Theta_{,l}v_{,l}$ and the divergence theorem yields the following expression

$$\int_{V_S}\left[\frac{\partial v}{\partial\tau_x}\frac{\partial\Theta}{\partial\tau_x}+\frac{\partial v}{\partial\tau_y}\frac{\partial\Theta}{\partial\tau_y}+\frac{\partial v}{\partial\tau_z}\frac{\partial\Theta}{\partial\tau_z}\right]\mathrm{d}V - \int_{\Gamma}v(\mathbf{x}-\mathbf{x}_i)\frac{\partial\Theta}{\partial n_w}\,\mathrm{d}\Gamma = -\int_{V_S}\left[\frac{(1-\omega)}{N_{\mathrm{CR}}}\left(\Theta^4-\frac{1}{4}\sum_{m=1}^{M}G^m w^m\right)\right]v(\mathbf{x}-\mathbf{x}_i)\,\mathrm{d}V \tag{34}$$

where Γ is the boundary of entire domain and n_w is the outward unit normal to the boundary Γ. Substitution of Eqs. (18)–(20) into Eq. (34) for all nodes leads to the following discretized system of linear equations:

$$\sum_{j=1}^{N}K_{ij}\Theta_j = f_i, \quad i=1,2,\ldots,N \tag{35}$$

where

$$K_{ij} = \int_{V_S}\left[\phi_{j,\tau_x}(\mathbf{x})v_{,\tau_x}(\mathbf{x}-\mathbf{x}_i)+\phi_{j,\tau_y}(\mathbf{x})v_{,\tau_y}(\mathbf{x}-\mathbf{x}_i) + \phi_{j,\tau_z}(\mathbf{x})v_{,\tau_z}(\mathbf{x}-\mathbf{x}_i)\right]\mathrm{d}V - \int_{\Gamma}\phi_{j,n_w}(\mathbf{x})v(\mathbf{x}-\mathbf{x}_i)\,\mathrm{d}\Gamma \tag{36}$$

$$f_i = -\int_{V_S}\left[\frac{(1-\omega)}{N_{\mathrm{CR}}}\left(\Theta^4-\frac{1}{4}\sum_{m=1}^{M}G^m w^m\right)\right]v(\mathbf{x}-\mathbf{x}_i)\,\mathrm{d}V \tag{37}$$

For each node i on the boundary, the dimensionless temperature Θ is given by Eq. (3), and the boundary condition can be directly imposed as follows:

$$K_{ij} = \begin{cases} 1, & i=j \\ 0, & i\neq j \end{cases} \tag{38}$$

$$f_i = \Theta_i \tag{39}$$

Because the energy equation contains the unknown radiative source and the radiative transfer equation contains unknown temperature, the global iterations are necessary to include radiation–conduction interactions. The implementation

of the MLPG method for solving the coupled radiative and conductive heat transfer can be carried out according to the following routine:

Step 1: Choose a finite number of nodes in the problem domain and its boundaries; decide the basis function, MLS weight function and test function such that the MLS approximation is well defined and the weighted integrations of the dimensionless energy equation and the dimensionless radiative transfer equation can be implemented.

Step 2: Determine the local sub-domain V_S and its boundary for each node, and calculate Gaussian quadrature points $\mathbf{x}_Q$ in V_S.

Step 3: Determine the nodes $\mathbf{x}_i$ located in the domain of definition of the MLS approximation for the trial function at point $\mathbf{x}_Q$, i.e., those nodes with $w_i(\mathbf{x}_Q) > 0$.

Step 4: For those nodes in the domain of definition of the MLS approximation of trial function at point $\mathbf{x}_Q$; calculate shape function $\phi_i(\mathbf{x}_Q)$ and the derivatives $\phi_{i,x}(\mathbf{x}_Q)$, $\phi_{i,y}(\mathbf{x}_Q)$, $\phi_{i,z}(\mathbf{x}_Q)$ and $\phi_{i,n_w}(\mathbf{x}_Q)$.

Step 5: Set the initial values of dimensionless temperature.

Step 6: Knowing the dimensionless temperatures, evaluate numerical integrals in Eqs. (29) and (30), assemble contributions to the linear system Eq. (28), and solve the set of linear equations for the fictitious nodal values of the dimensionless radiative intensities for all nodes.

Step 7: Knowing the dimensionless radiative intensities, evaluate numerical integrals in Eqs. (36) and (37), assemble contributions to the linear system Eq. (35), and solve the set of linear equations for the fictitious nodal values of the dimensionless temperatures for all nodes.

Step 8: Terminate the iteration process if the specified stopping criterion is satisfied. Otherwise, go back to step 6.

3. Results and discussions

To verify the meshless local Petrov–Galerkin approach for coupled radiative and conductive heat transfer, three particular test cases for coupled radiative and conductive heat transfer are examined. The particular test cases are selected because exact, or at least very precise, solutions of the coupled radiative and conductive heat transfer exist for comparison with the MLPG approach. A computer code based on the preceding calculation procedure was written. Node densification studies were also performed for the physical model to ensure that the essential physics are independent of node number. For the following numerical study, the equal weight even quadrature S_6 is selected, and Gaussian quadrature with 6 integration points in each coordinate is employed to evaluate numerical integrals in Eqs. (29), (30) and Eqs. (36), (37). The maximum relative error, 10^{-5}, of the dimensionless temperature or the dimensionless net wall heat flux is taken as the stopping criterion of iteration.

The dimensionless heat fluxes Q_x, Q_y and Q_z consist of both conduction and radiation. They are defined as follows

$$Q_x = \frac{q_x}{\sigma T_{\mathrm{ref}}^4} = -4N_{\mathrm{CR}}\frac{\partial \Theta}{\partial \tau_x} + \sum_{m=1}^{M} G^m \mu^m w^m \tag{40}$$

$$Q_y = \frac{q_y}{\sigma T_{\mathrm{ref}}^4} = -4N_{\mathrm{CR}}\frac{\partial \Theta}{\partial \tau_y} + \sum_{m=1}^{M} G^m \eta^m w^m \tag{41}$$

$$Q_z = \frac{q_z}{\sigma T_{\mathrm{ref}}^4} = -4N_{\mathrm{CR}}\frac{\partial \Theta}{\partial \tau_z} + \sum_{m=1}^{M} G^m \xi^m w^m \tag{42}$$

By using MLS approximation, the dimensionless heat fluxes defined in Eqs. (40)–(42) can be rewritten as

$$Q_x = -4N_{\mathrm{CR}}\sum_{i=1}^{n}\phi_{i,\tau_x}\Theta_i + \sum_{m=1}^{M} G^m \mu^m w^m \tag{43}$$

$$Q_y = -4N_{\mathrm{CR}}\sum_{i=1}^{n}\phi_{i,\tau_y}\Theta_i + \sum_{m=1}^{M} G^m \eta^m w^m \tag{44}$$

$$Q_z = -4N_{\mathrm{CR}}\sum_{i=1}^{n}\phi_{i,\tau_z}\Theta_i + \sum_{m=1}^{M} G^m \xi^m w^m \tag{45}$$

3.1. Case 1: One-dimensional non-scattering gray medium between parallel black plates

Consider the coupled radiative and conductive heat transfer in a layer of absorbing–emitting medium between parallel black plates at dimensionless temperatures Θ_0 and Θ_L. The medium between the plates is gray and has a constant thermal conductivity and absorption coefficient. The optical thickness of the layer is τ_L. The MLPG approach is applied to solve distribution of dimensionless temperatures and the profile of dimensionless heat fluxes in the layer. 51 nodes are uniformly distributed in the problem domain and its boundaries. The monomial basis $\mathbf{p}^T(\mathbf{x}) = [1, \tau_x, \tau_x^2]$ is used, and the weight function for the MLS approximation and the test function in the weighted integration of the dimensionless energy equation and the dimensionless radiative transfer equation are given as follows:

$$w^{\mathrm{MLS}}(\tau_x - \tau_{x_i}) = g_{\mathrm{qs}}\left(\left|\frac{\tau_x - \tau_{x_i}}{\alpha_{\mathrm{MLS}}\Delta\tau_x}\right|\right) \tag{46}$$

$$v(\tau_x - \tau_{x_i}) = g_{\mathrm{qs}}\left(\left|\frac{\tau_x - \tau_{x_i}}{\alpha_{\mathrm{GQ}}\Delta\tau_x}\right|\right) \tag{47a}$$

$$v_{\mathrm{sh}}(\tau_x - \tau_{x_i}) = g_{\mathrm{qs}}\left(\left|\frac{\tau_x - \tau_{x_i} + 0.5\mu^m\alpha_{\mathrm{GQ}}\Delta\tau_x}{[1 + 0.5\,\mathrm{sign}(\tau_x - \tau_{x_i})\mu^m]\alpha_{\mathrm{GQ}}\Delta\tau_x}\right|\right) \tag{47b}$$

where $\Delta\tau_x$ is the average nodal spacing between two neighbor nodes, and the dimensionless size parameters $\alpha_{\mathrm{MLS}} = 2.5$ and $\alpha_{\mathrm{GQ}} = 1.5$ are used.

The dimensionless temperature distributions are presented in Fig. 2 in the case of $\tau_L = 1.0$, $\Theta_0 = 1.0$ and $\Theta_L = 0.1$ for three different conduction to radiation parameters N_{CR}, namely, 0.01, 0.1, and 1.0, and are compared with the classical analytical solutions obtained by Viskanta and Grosh [1] and the solutions obtained by Burns et al. [6] using the quadratic Swartz–Wendroff approximation. The MLPG results agree with the solutions obtained by Viskanta and Grosh [1] and Burns et al. [6] very well. The maximum relative error of the dimensionless temperature based on the classical analytical solutions is

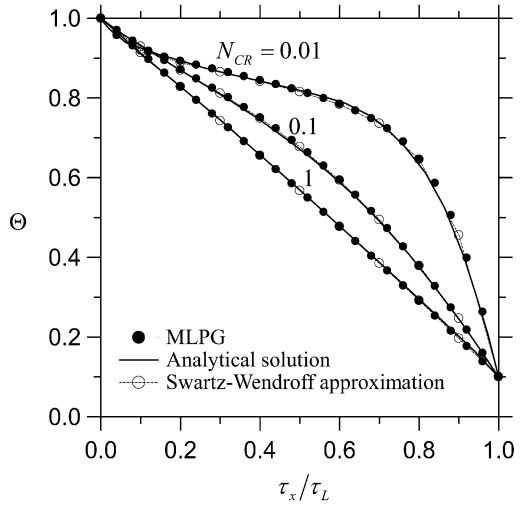

Fig. 2. Dimensionless temperature distributions in gray medium between infinite parallel black plates for the case of $\tau_L = 1.0$, $\Theta_0 = 1.0$ and $\Theta_L = 0.1$.

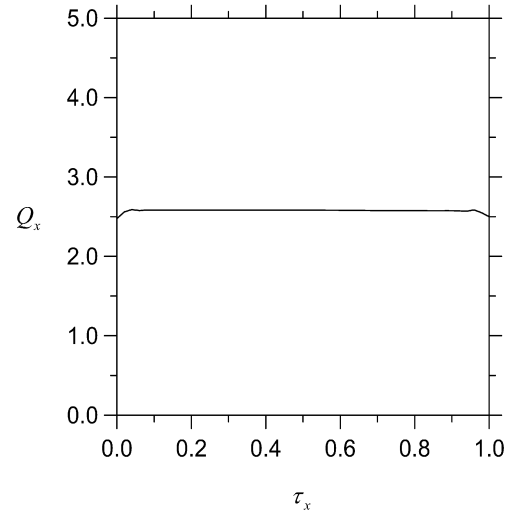

Fig. 3. MLPG approximation of the dimensionless heat fluxes based on different nodes in the case of $\tau_L = 1.0$, $N_{\mathrm{CR}} = 1.0$, $\Theta_0 = 1.0$ and $\Theta_L = 0.5$.

less than 1%. The time required for computation is less than 10 seconds on a personal computer with Intel Pentium Pro 450 MHz processor. The convergence, CPU time and memory requirements are of the same order of magnitude as that of finite element method. However, meshless methods are competitive for the problem with change of geometry shape, for example, the inverse design of geometry shape, in which meshing and re-meshing are needed with the change of the geometry shape. At that time, for mesh-based method, such as FEM, meshing and re-meshing are difficult task.

The MLPG approximation of the dimensionless heat fluxes based on different nodes within the layer are profiled in Fig. 3 in the case of $\tau_L = 1.0$, $N_{\mathrm{CR}} = 1.0$, $\Theta_0 = 1.0$ and $\Theta_L = 0.5$. Theoretically, the exact dimensionless heat flux is a constant in this case, but the computed values of dimensionless heat flux by using MLPG approach vary with the location of nodes. This is because that, the dimensionless heat flux contains the information concerning the derivatives of variables, but the moving least squares approximation is based only on the information of the values of variables at some nodes and the derivative information is not used to construct the conventional MLPG approximation solution. However, even in this case the averaged dimensionless heat flux computed by using MLPG approach, 2.575, is very close to the exact value, namely, 2.600. The maximum relative error of the dimensionless heat flux is less than 4%.

Table 1
Dimensionless heat fluxes in the case of $\Theta_0 = 1.0$ for different values of τ_L, Θ_L and N_{CR}

τ_L	Θ_L	N_{CR}	Dimensionless heat flux	
			Ref. [2]	MLPG
0.1	0.5	0.01	1.074	1.101
0.1	0.5	0.1	2.880	2.900
0.1	0.5	1	20.88	20.89
0.1	0.5	10	200.88	200.79
1	0.5	0.01	0.596	0.571
1	0.5	0.1	0.798	0.773
1	0.5	1	2.600	2.575
1	0.5	10	20.60	20.56
1	0.1	0.01	0.658	0.635
1	0.1	0.1	0.991	0.972
1	0.1	1	4.218	4.198
1	0.1	10	36.60	36.57
10	0.5	0.01	0.114	0.113
10	0.5	0.1	0.131	0.133
10	0.5	1	0.315	0.315
10	0.5	10	2.114	2.113

The averaged dimensionless heat fluxes in the case of $\Theta_0 = 1.0$ for different values of τ_L, Θ_L and N_{CR} are computed by using MLPG approach and given in Table 1. The results are compared with those obtained by Viskanta and Grosh [2] using numerical integration and iteration. From Table 1, it can be seen that the MLPG approach presented in this paper has a good accuracy in solving the dimensionless heat fluxes in one-dimensional non-scattering gray medium. The maximum relative error of the dimensionless heat flux is less than 4.5%.

3.2. Case 2: One-dimensional scattering gray medium between parallel diffuse gray plates

In this case, we consider the coupled radiative and conductive heat transfer in a layer of absorbing, emitting, and scattering medium between parallel diffuse plates. The medium and the plates are gray. The following linear phase function is used:

$$\Phi(\mu, \mu') = 1 + g\mu\mu' \tag{48}$$

The MLPG approach is applied to solve the distribution of dimensionless temperatures and the profile of dimensionless heat fluxes in the layer. The nodal number, the monomial basis and the weight function for the MLS approximation and the test function are same as Case 1. The dimensionless heat flux in the case of $\tau_L = 1.0$, $\varepsilon_0 = \varepsilon_L = 1.0$, $\omega = 1.0$, $\Theta_0 = 1.0$ and $\Theta_L = 0.5$ for different values of N_{CR} and g are given in Table 2, and compared with the results obtained by Yuen and Wong [3] using a successive approximation technique. MLPG results are very close to the values obtained by Yuen and Wong.

Table 2
Dimensionless heat flux in the case of $\tau_L = 1.0$, $\varepsilon_0 = \varepsilon_L = 1.0$, $\omega = 1.0$, $\Theta_0 = 1.0$ and $\Theta_L = 0.5$ for different values of N_{CR} and g

N_{CR}	g	Dimensionless heat flux	
		Ref. [3]	MLPG
1.0	1.0	2.602	2.577
1.0	0.0	2.519	2.491
1.0	−1.0	2.456	2.425
0.01	1.0	0.622	0.627
0.01	0.0	0.539	0.542
0.01	−1.0	0.476	0.479

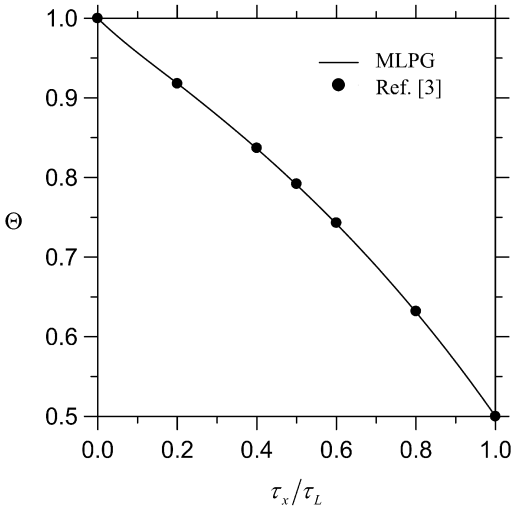

Fig. 4. Dimensionless temperature profile in a layer of absorbing, emitting, and scattering medium between parallel diffuse plates for the case of $N_{CR} = 1.0$, $\tau_L = 10.0$, $\varepsilon_0 = \varepsilon_L = 1.0$, $\Theta_0 = 1.0$, $\Theta_L = 0.5$, $\omega = 0.5$ and $g = 1.0$.

The maximum relative error of the dimensionless heat flux is less than 2%.

The dimensionless temperature profile in the case of $N_{CR} = 1.0$, $\tau_L = 10.0$, $\varepsilon_0 = \varepsilon_L = 1.0$, $\Theta_0 = 1.0$ and $\Theta_L = 0.5$, $\omega = 0.5$ and $g = 1.0$ is shown in Fig. 4, and compared with the results obtained by Yuen and Wong [3]. No observable difference could be detected between the MLPG results and the values obtained by Yuen and Wong [3] when the results are presented in graphical form.

3.3. Case 3: Two-dimensional absorbing–emitting media in a Black Enclosure

As shown in Fig. 5, we consider the coupled radiative and conductive heat transfer in a two-dimensional rectangular gray semitransparent media enclosed by black boundaries. The optical thickness based on the side length L of rectangular enclosure is $\tau_L = \beta L = 1.0$. The dimensionless temperature of the left-hand wall is maintained at 1.0 with other walls at 0.5.

The MLPG approach is applied to solve the distribution of dimensionless temperatures and the profile of dimensionless heat fluxes in the two-dimensional enclosure. As shown in Fig. 5, 441 nodes are uniformly distributed in the problem domain and its boundaries. The monomial basis $\mathbf{p}^T(\mathbf{x}) = [1, \tau_x, \tau_y, \tau_x^2, \tau_x\tau_y, \tau_y^2]$ is used, and the weight function for the

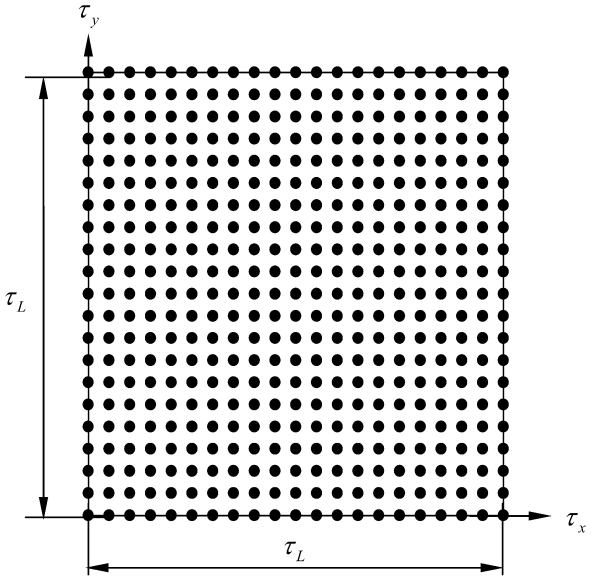

Fig. 5. Two-dimensional rectangular geometry and the distribution of nodes.

MLS approximation and the test function in the weighted integration of the dimensionless energy equation and the dimensionless radiative transfer equation are given as follows:

$$w^{\mathrm{MLS}}(\mathbf{x} - \mathbf{x}_i) = w\left(\left|\frac{\tau_x - \tau_{x_i}}{\alpha_{\mathrm{MLS}}\Delta\tau_x}\right|\right) w\left(\left|\frac{\tau_y - \tau_{y_i}}{\alpha_{\mathrm{MLS}}\Delta\tau_y}\right|\right) \tag{49}$$

$$v(\mathbf{x} - \mathbf{x}_i) = w\left(\left|\frac{\tau_x - \tau_{x_i}}{\alpha_{\mathrm{GQ}}\Delta\tau_x}\right|\right) w\left(\left|\frac{\tau_y - \tau_{y_i}}{\alpha_{\mathrm{GQ}}\Delta\tau_y}\right|\right) \tag{50a}$$

$$v_{\mathrm{sh}}(\mathbf{x} - \mathbf{x}_i) = g_{\mathrm{qs}}\left(\left|\frac{\tau_x - \tau_{x_i} + 0.5\mu^m\alpha_{\mathrm{GQ}}\Delta\tau_x}{[1 + 0.5\,\mathrm{sign}(\tau_x - \tau_{x_i})\mu^m]\alpha_{\mathrm{GQ}}\Delta\tau_x}\right|\right) \times g_{\mathrm{qs}}\left(\left|\frac{\tau_y - \tau_{y_i} + 0.5\eta^m\alpha_{\mathrm{GQ}}\Delta\tau_y}{[1 + 0.5\,\mathrm{sign}(\tau_y - \tau_{y_i})\eta^m]\alpha_{\mathrm{GQ}}\Delta\tau_y}\right|\right) \tag{50b}$$

where $\Delta\tau_x$ and $\Delta\tau_y$ are the average nodal spacing between two neighbor nodes in τ_x and τ_y coordinate directions, respectively, and the dimensionless size parameters $\alpha_{\mathrm{MLS}} = 2.5$ and $\alpha_{\mathrm{GQ}} = 1.5$ are used.

The profiles of the dimensionless temperatures and the dimensionless heat fluxes along the symmetry line at $\tau_y = 0.5$ for the case of $N_{CR} = 1.0$ are shown in Figs. 5 and 6, respectively, and compared to the results obtained by Yuen and Takara [7]. By comparison, it can be seen that the MLPG approach has a good accuracy in solving the coupled radiative and conductive heat transfer in two-dimensional semitransparent media. The MLPG results are very close to those obtained by Yuen and Takara [7]. Similar to Case 2, for the profile of the dimensionless temperature, no observable difference could be detected between the MLPG results and the values obtained by Yuen and Takara [7] when the results are presented in graphical form. However, there exist some errors of the dimensionless heat flux in the zone close to the left-hand wall. Even in this case, the maximum relative error of MLPG approximation for the dimensionless heat flux is less than 3%.

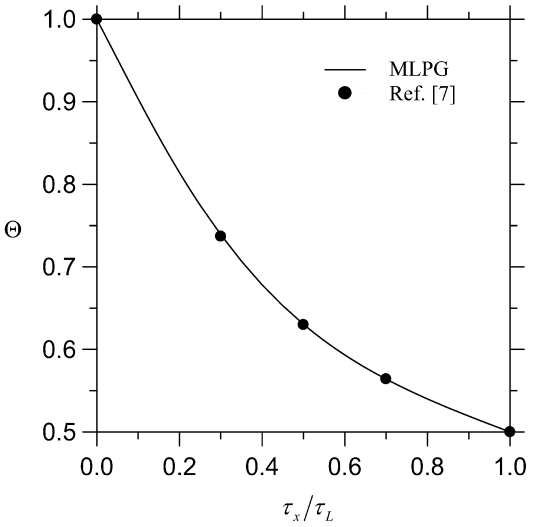

Fig. 6. Dimensionless temperature profile along the symmetry line at $\tau_y = 0.5$.

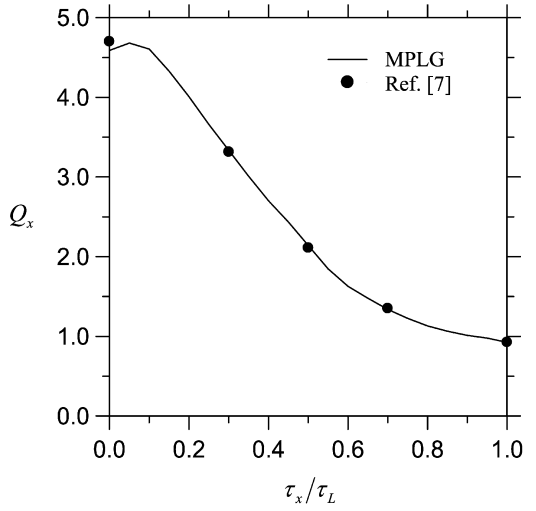

Fig. 7. Dimensionless heat flux profile along the symmetry line at $\tau_y = 0.5$.

4. Conclusions

A MLPG approach is employed for solving the coupled radiative and conductive heat transfer in absorbing, emitting and scattering media. The meshless local Petrov–Galerkin approach with upwind scheme for radiative transfer is based on the discrete ordinate equations. The moving least square approximation is used to construct the shape function. Three particular test cases for coupled radiative and conductive heat transfer are examined to verify this new approximate method. The dimensionless temperatures and the dimensionless heat fluxes are obtained. The results are compared with the other benchmark approximate solutions. The results show that the MLPG approach has a good accuracy in solving the coupled radiative and conductive heat transfer in absorbing, emitting and scattering media. In comparison with the traditional numerical method, such as, finite volume method, finite element method and so on, the MLPG approach avoids the complex and time-consuming meshing and re-meshing processes and can be used to solve the coupled radiative and conductive heat transfer in multi-dimensional absorbing, emitting and scattering media.

Acknowledgements

The support of this work by the National Nature Science Foundation of China (50425619, 50336010, 50576018) is gratefully acknowledged.

References

[1] R. Viskanta, R.J. Grosh, Heat transfer by simultaneous conduction and radiation in an absorbing medium, Journal of Heat Transfer 84 (1962) 63–72.
[2] R. Viskanta, R.J. Grosh, Effect of surface emissivity heat transfer by simultaneous conduction and radiation, International Journal of Heat and Mass Transfer 5 (1962) 729–734.
[3] W.W. Yuen, L.W. Wong, Heat transfer by conduction and radiation in a one-dimensional absorbing, emitting and anisotropically-scattering medium, Journal of Heat Transfer 102 (1980) 303–307.
[4] I.E. Enoch, E. Ozil, R.C. Birkebak, Polynomial approximation solution of heat transfer by conduction and radiation in a one-dimensional absorbing, emitting, and scattering medium, Numerical Heat Transfer 5 (1982) 353–358.
[5] M.L. Nice, Applications of finite elements to heat transfer in a participating medium, in: T.M. Shih (Ed.), Numerical Properties and Methodologies in Heat Transfer, Hemisphere, Washington, DC, 1983, pp. 497–514.
[6] S.P. Burns, J.R. Howell, D.E. Klien, Empirical evaluation of an important approximation for combined-mode heat transfer in a participating medium using the finite element method, Numerical Heat Transfer, Part B 27 (1995) 309–322.
[7] W.W. Yuen, E.E. Takara, Analysis of combined conductive–radiative heat transfer in a two-dimensional rectangular enclosure with a gray medium, Journal of Heat Transfer 110 (1988) 468–474.
[8] M.M. Razzaque, J.R. Howell, D.E. Klein, Coupled radiative and conductive heat transfer in a two-dimensional rectangular enclosure with gray participating media using finite elements, Journal of Heat Transfer 106 (1984) 613–619.
[9] T.Y. Kim, S.W. Baek, Analysis of combined conductive and radiative heat transfer in a two-dimensional rectangular enclosure using the discrete ordinates method, International Journal of Heat and Mass Transfer 34 (1991) 2265–2273.
[10] M.F. Modest, Radiative Heat Transfer, second ed., Academic Press, San Diego, CA, 2003.
[11] R. Siegel, J.R. Howell, Thermal Radiation Heat Transfer, fourth ed., Taylor & Francis, Washington, DC, 2002.
[12] S.V. Patankar, Numerical Heat Transfer and Fluid Flow, Hemisphere, New York, 1980.
[13] J.N. Reddy, D.K. Gartling, The Finite Element Method in Heat Transfer and Fluid Dynamics, second ed., CRC Press, Boca Raton, FL, 2001.
[14] G.R. Liu, Mesh Free Methods, CRC Press, Boca Raton, FL, 2003.
[15] X. Zhang, Y. Liu, Meshless Methods, Tsinghua Univ. Press, Beijing, 2004.
[16] S.N. Atluri, S.P. Shen, The Meshless Local Petrov–Galerkin (MLPG) Method, Tech Science Press, Encino, 2002.
[17] S.N. Atluri, T. Zhu, A new meshless local Petrov–Galerkin (MLPG) approach in computational mechanics, Computational Mechanics 22 (1998) 117–127.
[18] I.V. Singh, K. Sandeep, R. Prakash, Heat transfer analysis of two-dimensional fins using a meshless element free Galerkin method, Numerical Heat Transfer A 44 (2003) 73–84.
[19] L.H. Liu, Meshless local Petrov–Galerkin method for solving radiative transfer equation, Journal of Thermophysics and Heat Transfer 20 (2006) 150–154.
[20] L.H. Liu, Meshless method for radiative heat transfer in graded index medium, International Journal of Heat and Mass Transfer 49 (2006) 219–229.

[21] L.H. Liu, J.Y. Tan, B.X. Li, Meshless approach for coupled radiative and conductive heat transfer in one-dimensional graded index medium, Journal of Quantitative Spectroscopy & Radiative Transfer 101 (2006) 237–248.
[22] H. Sadat, On the use of a meshless method for solving radiative transfer with the discrete ordinates formulations, Journal of Quantitative Spectroscopy & Radiative Transfer 101 (2006) 263–268.
[23] L.H. Liu, H.P. Tan, Numerical Simulation of Thermal Radiative Transfer in Graded Index Medium, Science Press, Beijing, 2006.
[24] J.C. Chai, S.V. Patankar, Finite-volume method for radiation heat transfer, in: W.J. Minkowycz, E.M. Sparrow (Eds.), Advances in Numerical Heat Transfer, vol. 2, Taylor & Francis, New York, 2000, pp. 109–141.
[25] H. Lin, S.N. Atluri, Meshless local Petrov–Galerkin (MLPG) method for convection–diffusion problems, Computer Modeling in Engineering and Sciences 1 (2000) 45–60.
[26] J.C. Chai, H.S. Lee, S.V. Patankar, Improved treatment of scattering using the discrete ordinates method, Journal of Heat Transfer 166 (1994) 260–263.